Supporting Information:

Aggravated toxicity of copper sulfide nanoparticles via hypochlorite-induced nanoparticle dissolution

Long Kong[1, 2], Xiaohong Wang[1]*, Xiaoyu Li[1], Jian Liu[1], Xinxin Huang[1], Yingju Qin[1], Xin Che[1], Hongyu Zhou[1]*, Christopher J. Martyniuk[3], Bing Yan[1, 2]

[1] Institute of Environmental Research at Greater Bay Area; Key Laboratory for Water Quality and Conservation of the Pearl River Delta, Ministry of Education, Guangzhou University, Guangzhou 510006, China

[2] School of Environmental Science and Engineering, Shandong University, Jinan, Shandong, 250100, China

[3] Center for Environmental and Human Toxicology, Department of Physiological Sciences, College of Veterinary Medicine, UF Genetics Institute, Interdisciplinary Program in Biomedical Sciences in Neuroscience, University of Florida, Gainesville, Florida, 32611, USA

Characterization of CuSNPs

For characterization of the prepared CuSNPs, transmission electron microscopy (TEM, Hitachi H-7500, Tokyo, Japan) was used to measure the morphology and size of the material. The hydrodynamic size and zeta potential of CuSNPs were calculated from the average of three measurements using dynamic light scattering (DLS, Malvern, United Kingdom). The X-ray diffraction analysis (XRD) analysis was carried out with a Germany Bruker D2 Phaser rotation anode X-ray diffractometer, using Cu-Ka radiation at 25℃. A scanning rate of 0.02°/0.5s was applied to record the patterns in the 2θ range 10-80°. The reflection data were collected at 25 ℃. For characterization of the CuSNPs disinfected by hypochlorite, we mixed the CuSNPs and free chlorine solutions, and obtained a mixture with final concentrations of 200 μg/L CuSNPs and 4 mg/L hypochlorite. The mixture was slowly shaken for 24 h and then characterized by using TEM, DLS, and XRD. In order to identify the conversion before and after CuSNPs oxidation, the X-ray photoelectron spectroscopy (XPS) high-resolution spectra of CuSNP dry powders were recorded by X-ray photoelectron spectrometer (XPS, Escalab 250xi, Thermo Fisher Inc. ,America). XPS data is analyzed by XPS PEAK Fit v4.1 software.

Breeding of zebrafish embryos

Wildtype zebrafish (AB-strain) were obtained from the Zebrafish Resource Center (Wuhan, China), and maintained at ~28 ºC with 14 h light and10 h dark photoperiod, for at least two weeks in our lab's flow-through rearing system (Zhongwei Purification Mechanical and Electrical Engineering Co. Ltd, Guangzhou, China). The male- and female- zebrafish were separately maintained and fed with brine shrimp three times each day. Zebrafish embryos were obtained from adult fish by organizing individuals

at a ratio of 1 female and 3 males in the spawning box in the evening before egg collections. Zebrafish eggs were collected the next morning, and placed into embryo rearing medium (ERM)[1] for exposure experiments. Double distilled water was used to prepare ERM. The components of each liter of ERM contain NaCl (800 mg), KCl (40 mg), Na2HPO4 (3.5 mg), KH2PO4 (60 mg), CaCl2 (14 mg), MgSO4 (12 mg), and NaHCO3 (35 mg).

Copper accumulation in fish embryos

The experimental protocols were approved by Guangzhou University Institutional Animal Care and Use Committee, following the "Guide for the care and use of laboratory animals" proposed by the National Institutes of Health. Ten zebrafish embryos were cultured in a 24-well plate with 6 replicates for each treatment. They were exposed to either embryo raising medium (ERM), CuSNPs, hypochlorite, the mixture of CuSNPs and hypochlorite, or the dissolved copper, respectively at indicated concentrations. After exposure, each sample was washed with ultrapure water 3 times, and collected in a 1.5 mL centrifuge tube. The residual water was removed, and 200 μL nitric acid (70%) was added to each sample prior to being digested in a microwave oven. After dilution with ultrapure water, copper contents in the digested solutions were analyzed using ICP-MS.

Detection of metallothionein levels

To evaluate responses to copper taken up into zebrafish, metallothionein (MT) (a molecular marker for metal exposure) was measured using a commercial kit from Nanjing Jiancheng Bioengineering Institute. Fish were cultured in 12-well plates with 30 fish per well. Fish exposed to either ERM or one of the experimental treatments were done in triplicate. At the end of 96 h exposure, all surviving fish from one well

were collected as one sample. The zebrafish were euthanized and fully lysed, collected and added into assay wells pre-coated with antibodies. Following this, recognition antigen labelled by horseradish peroxidase (HRP) was added. After 30 min incubation, tetramethyl benzidine (TMB, 50 μL) was added and signal at 450 nm was measured using a microplate reader (BioTek Instruments, Inc. Vermont, USA).

The operational details of UHPLC-Q-TOF for metabolomics

The instrument was operated as previously reported.[2] For UHPLC separation, samples were analyzed using a 2.1 × 100 mm ACQUITY UPLC BEH 1.7 μm column (Waters, Ireland). In both ESI positive and negative modes, the mobile phase A contained 25 mM CH_3COONH_4 and 25 mM $NH_3 \cdot H_2O$ in water, while mobile phase B was acetonitrile.[3] The gradient was 85% acetonitrile for 1 min which was linearly reduced to 65% in 11 min, further reduced to 40% in 0.1 min and kept for 4 min, and then increased to 85% in 0.1 min, with a 5 min re-equilibration period employed. The ESI source conditions in Q-TOF were set as follows: Ion Source Gas 1 (Gas 1): 60, ion Source Gas 2 (Gas 2): 60, Curtain Gas (CUR): 30, source temperature: 600 ºC, ionSapary Voltage Floating (ISVF): ± 5500 V. In MS-acquisition only mode, the instrument was set to acquire over the m/z range 60-1000 Da, and the accumulation time for TOF MS scan was set at 0.20 s/spectra. In auto MS/MS acquisition, the instrument was set to acquire data over the m/z range 25-1000 Da, and the accumulation time for the product ion scan was set at 0.05 s/spectra. The product ion scan was acquired using information dependent acquisition (IDA) with the high sensitivity mode selected. The collision energy (CE) was fixed at 35 V with ± 15 eV. Declustering potential (DP) was set at ± 60 V.

Real-time PCR analysis

Approximately 10 zebrafish from each well were pooled as one sample for

transcript analysis (N = 4) after exposure to each of the treatments., RNApre Pure Tissue Kit (Tiangen Biotech, Beijing, China) was used for extraction of total RNA, the quantity and quality of which were determined by a NanoDrop One spectrophotometer (ThermoFisher Scientific, USA). For cDNA synthesis, 2 μg of purified RNA was processed using the PrimeScript™ RT Master Mix (Takara, Japan). Real-time quantitative PCR assay was conducted by using the Roche LightCycler® 96 System with TaKaRa TB Green™ Premix Ex Taq™ II. The cycling parameters were set as 50 ºC for 2 min, 95 ºC for 5 min, 40 cycles of 94 ºC for 15 s, and 60 ºC for 30 s. The genes investigated included transcription factors pregnane X receptor (*pxr*), peroxisome proliferator-activated receptors (*pparα*, *pparβ*), and nuclear factor-erythroid 2-related factor-2 (*nrf2*), because they were important modulators of ABC transporters in zebrafish. Expression of multidrug resistance associated proteins (*mrp1*, *mrp2*) and p-glycoprotein (*pgp*) were also investigated, as they were important ABC transporters in the detoxification of heavy metals. Geometric mean of the two housekeeping genes (*ribosomal subunit 18* (*rps18*) *and Ribosomal protein L13a* (*rpl13a*)) were used to normalize the expression of target genes. The sequence of primer sets for target genes were shown in Table S1. The relative ΔΔCq method outlined by Pfaffl was adapted to evaluate the normalized gene expression.[4]

Data processing

ProteoWizard MSConvert was used to convert Raw MS data to MzXML files. Feature detection, retention time correction and alignment were then performed using XCMS.[5] MS/MS data were matched with standards database and the metabolites by accuracy mass (< 25 ppm) were identified. MetaboAnalyst (www.metaboanalyst.ca) web-based system was used for the multivariate statistical analysis. Principal component analysis (PCA) and partial least-squares-discriminant analysis (PLS-DA)

were performed using SIMCA-P 14.1 (Umetrics, Umea, Sweden). Significant differences of metabolites among experimental groups were determined based on the combination of variable influence on projection (VIP) values obtained from PLS-DA model and two-tailed Student's t test (*p* value) on the raw data. Metabolites with VIP values > 1.0 and *p* values < than 0.05 were considered as significant.

For hierarchical clustering analysis, Cluster 3.0 software was used for the selected metabolites.[6] Heatmaps were generated by Java Treeview software. The metabolites were blasted against the online Kyoto Encyclopedia of Genes and Genomes (KEGG) database (http://geneontology.org/) to retrieve their COs and were mapped to pathways in KEGG. The KEGG pathway enrichment analyses were applied based on the Fisher' exact test. Only pathways with p-values < 0.05 were considered significantly different between groups.

Data analysis

Experimental results were presented as mean values with standard error. The differences between exposure groups from zebrafish *in vivo* experiments were analyzed with One-way ANOVA followed by a Tukey's post hoc test. Values of $p < 0.05$ were judged to indicate statistical differences among groups. The statistical analysis and supporting figures were prepared using GraphPad Prism 8.0 (GraphPad Software Inc., La Jolla, CA, USA).

Reference：

1. M. Westerfield, A guide for the laboratory use of zebrafish (*Danio rerio*) Eugene, 2000, **1**, 10-16.
2. T. Du, Z. Lin, Y. Xie, X. Ye, C. Tu, K. Jin, J. Xie and Y. Shen, Metabolic profiling of femoral muscle from rats at different periods of time after death, *PLoS One*, 2018, **13**, e0203920.
3. W. Lan, Y. Ren, Z. Wang, J. Liu and H. Liu, Metabolic Profile Reveals the Immunosuppressive Mechanisms of Methionyl-Methionine in

Lipopolysaccharide-Induced Inflammation in Bovine Mammary Epithelial Cell, *Animals*, 2021, **11**, 833.

4. M. W. Pfaffl, A new mathematical model for relative quantification in real-time RT–PCR, *Nucleic Acids Res.*, 2001, **29**, e45.
5. R. Adusumilli and P. Mallick, in *Proteomics: Methods and Protocols*, eds. L. Comai, J. E. Katz and P. Mallick, Springer New York, New York, NY, 2017, DOI: 10.1007/978-1-4939-6747-6_23, pp. 339-368.
6. Y. Cao, Y. Zhou, D. Chen, R. Wu, L. Guo and H. Lin, Proteomic and metabolic characterization of membrane vesicles derived from Streptococcus mutans at different pH values, *Appl. Microbiol. Biotechnol.*, 2020, **104**, 9733-9748.

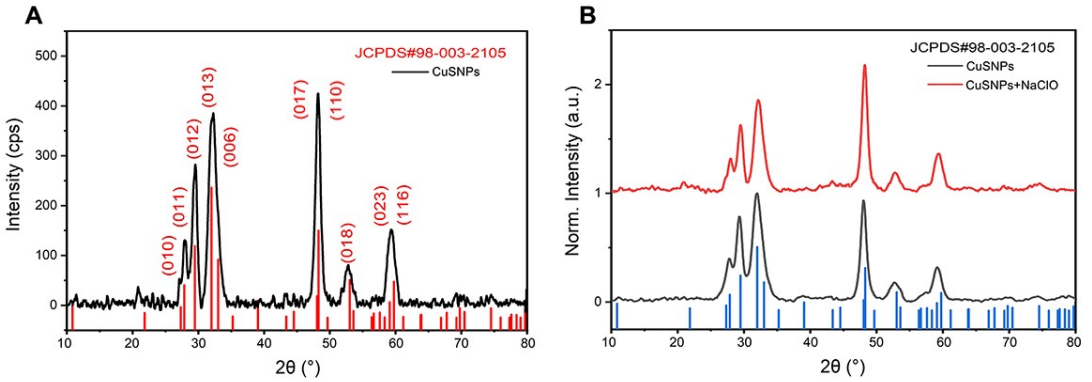

Fig. S1. XRD pattern of (A) the prepared CuSNPs and (B) CuSNPs before and after 24 h hypochlorite oxidation.

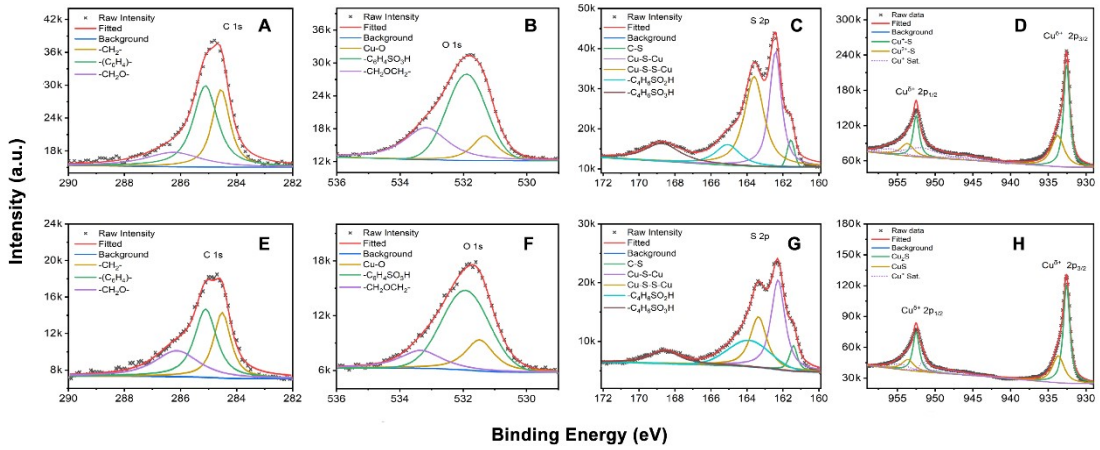

Fig. S2. High resolution XPS spectra of CuSNPs (A-D) before and (E-H) after 24 h hypochlorite oxidation. (A, E) C 1s spectra, (B, F) O 1s spectra, (C, D) S 2p spectra, and (D, H) Cu 2p spectra.

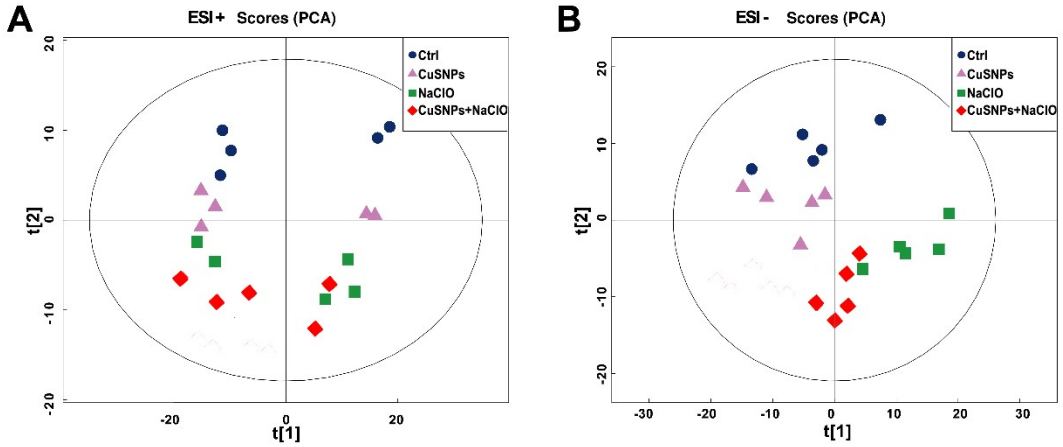

Fig. S3. Multivariate analysis of metabolomics data in zebrafish. PCA score plots of metabolomics data in the control, CuSNPs, hypochlorite, mixture of CuSNPs and hypochlorite groups in (A) positive and (B) negative ionization modes.

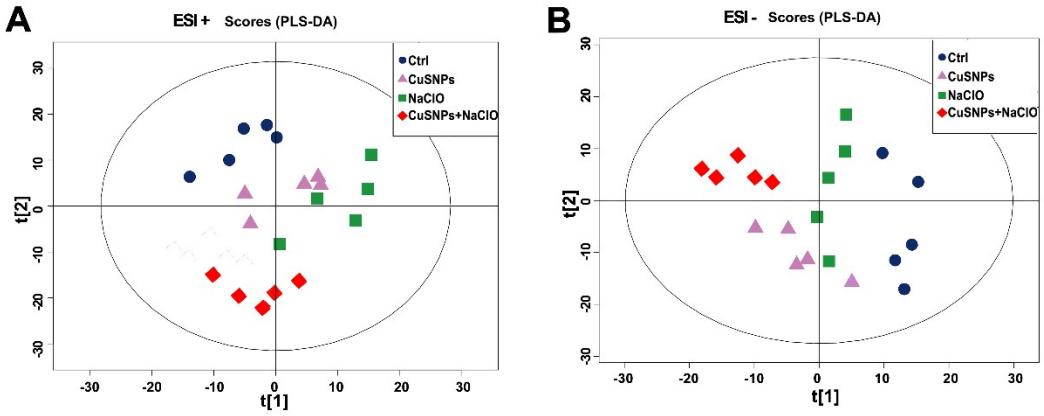

Fig. S4. Multivariate analysis of metabolomics data in zebrafish. PLS-DA score plots of metabolomics data in the control, CuSNPs, hypochlorite, mixture of CuSNPs and hypochlorite groups in (A) positive and (B) negative ionization modes.

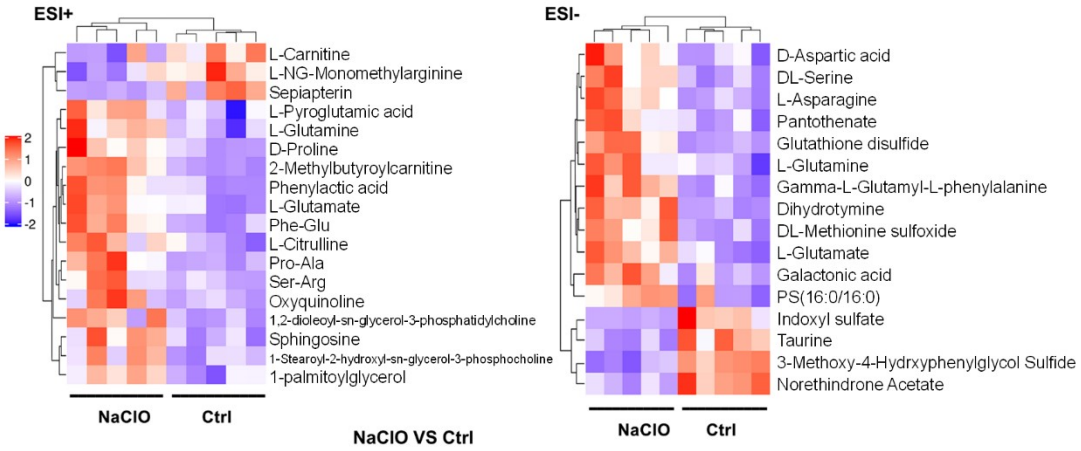

Fig. S5. Hierarchical clustering analysis of metabolomics data in zebrafish. Heatmaps for differentially expressed metabolites between hypochlorite exposure and control groups in both positive and negative ionization modes.

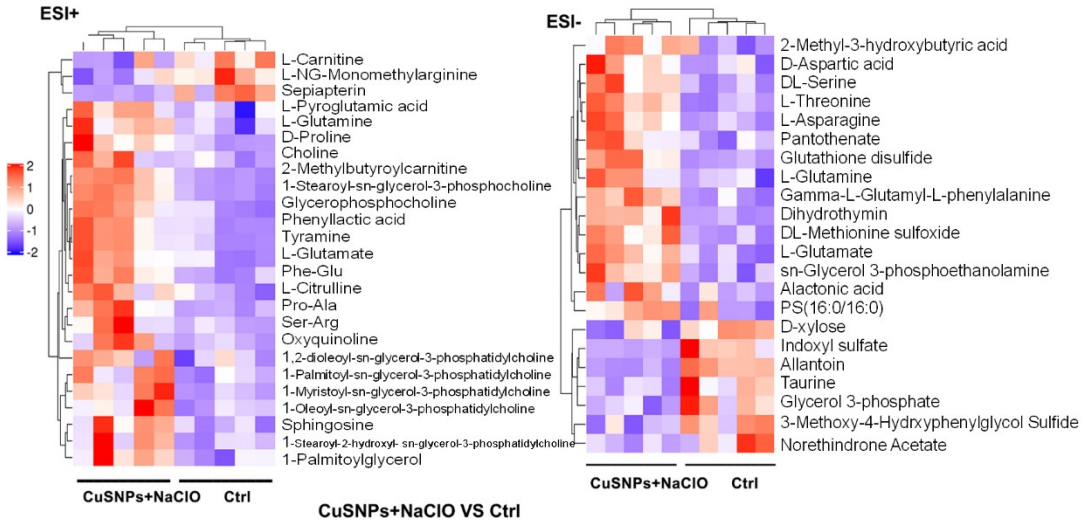

Fig. S6. Hierarchical clustering analysis of metabolomics data in zebrafish. Heatmaps for differentially expressed metabolites between the mixture exposure and control groups in both positive and negative ionization modes.

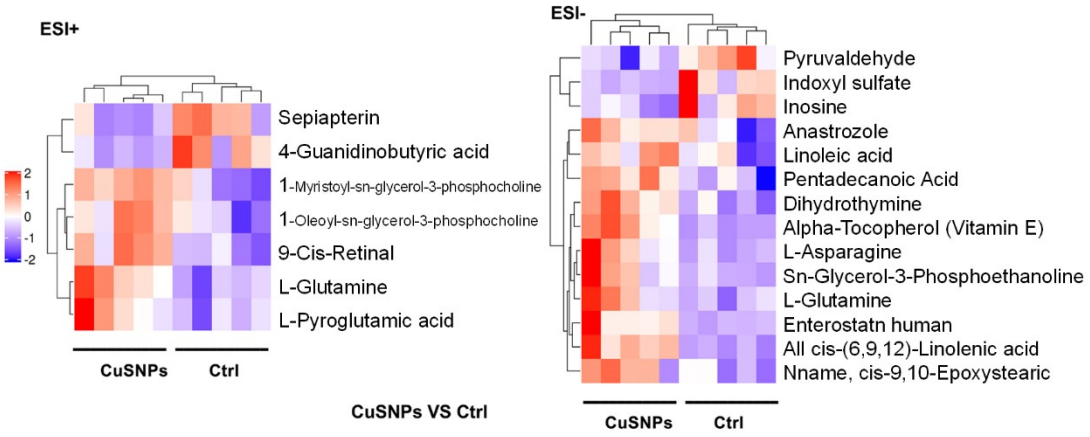

Fig. S7. Hierarchical clustering analysis of metabolomics data in zebrafish. Heatmaps for differentially expressed metabolites between CuSNPs exposure and control groups in both positive and negative ionization modes.

Table S1. Primers used for real-time PCR analysis

Symbol	Gene Name	Forward Primer (5'-3')	Reverse Primer (5'-3')
[a]*rps18*	Ribosomal protein S18	TCGCTAGTTGGCATCGTTTATG	CGGAGGTTCGAAGACGATCA
[a]*rpl13a*	Ribosomal protein L13a	AGCTCAAGATGGCAACACAG	AAGTTCTTCTCGTCCTCC
[b]*pxr*	Pregnane X receptor	CCGACTACAGAAGTGCCTCTC	CAGGCTCTTCCTGCATCCTC
[b]*nrf2*	Nuclear factor-erythroid 2-related factor-2	TCACTCCCAGAGTTGCAGCAG	TGTTTGAGCCGAGCCGAGA
[b]*ppar-α*	Peroxisome proliferator-activated receptor alpha	TTCAGCAGGAACAGCTTGTCT	GACGAGGGACTGTAGAGGCT
[b]*ppar-β*	Peroxisome proliferator-activated receptor beta	TCCTGACGGGAAAGACAAGC	AATATGCGCACCTCAGGGTC
[b]*mrp1*	Multidrug resistance associated proteins, member 1	CAGTCCACCATCCGAACTCA	GAACAGGCTCTACAGCCCAC
[b]*mrp2*	Multidrug resistance associated proteins, member 2	ACCGTCCGTTTTATCCGGTC	TCGAAGGATGTTTCCCAGGC
[b]*pgp*	P-glycoprotein	TCGTCATCCTCGCTGTTAGC	ATGACAGCACTTCCTCTGCC

[a]Wang, X.H., Souders II, C.L., Zhao, Y.H. and Martyniuk, C.J. (2018) Paraquat affects mitochondrial bioenergetics, dopamine system expression, and locomotor activity in zebrafish (Danio rerio). Chemosphere. 191, 106-117.

[b]Tian, J., Hu, J., Liu, G., Yin, H., Chen, M., Miao, P., Bai, P. and Yin, J. (2019) Altered Gene expression of ABC transporters, nuclear receptors and oxidative stress signaling in zebrafish embryos exposed to CdTe quantum dots. Environmental pollution. 244, 588-599.

Table S2. The identified metabolic pathways that are significantly changed between CuSNPs and control.

Pathway names	Hits	Metabolites	Category
Alanine, aspartate and glutamate metabolism	2	L-Asparagine; L-Glutamine	Amino acid metabolism
Aminoacyl-tRNA biosynthesis	2	L-Asparagine; L-Glutamine	Translation
Biosynthesis of unsaturated fatty acids	2	all cis-(6,9,12)-Linolenic acid; Linoleic acid	Lipid metabolism
Linoleic acid metabolism	2	all cis-(6,9,12)-Linolenic acid; Linoleic acid	Lipid metabolism

Table S3. The identified metabolic pathways that are significantly changed between the mixture exposure of CuSNPs and hypochlorite and control.

Pathway names	Hits	Metabolites	Category
Aminoacyl-tRNA biosynthesis	4	DL-Serine; L-Asparagine; L-Glutamate; L-Glutamine; L-Threonine	Translation
ABC transporters	8	Choline; DL-Serine; D-Xylose; Glycerol 3-phosphate; Taurine; L-Glutamate; L-Glutamine; L-Threonine	Membrane transport
Biosynthesis of amino acids	6	DL-Serine; L-Asparagine; L-Citrulline; L-Glutamate; L-Glutamine; L-Threonine	Global and overview maps
Glycerophospholipid metabolism	4	Choline; Glycerol 3-phosphate; Glycerophosphocholine; sn-Glycerol 3-phosphoethanolamine	Lipid metabolism
Alanine, aspartate and glutamate metabolism	4	D-Aspartic acid; L-Asparagine; L-Glutamate; L-Glutamine	Amino acid metabolism
Glycine, serine and threonine metabolism	4	DL-Serine; DL-Serine; Choline; L-Threonine	Amino acid metabolism
Arginine biosynthesis	3	L-Citrulline; L-Glutamate; L-Glutamine	Amino acid metabolism
Glutathione metabolism	3	Glutathione disulfide; L-Glutamate; L-Pyroglutamic acid	Amino acid metabolism
D-Glutamine and D-glutamate metabolism	2	L-Glutamate; L-Glutamine	Amino acid metabolism
Neuroactive ligand-receptor interaction	3	L-Glutamate; Taurine; Tyramine	Signaling molecules and interaction
Nitrogen metabolism	2	L-Glutamate; L-Glutamine	Energy metabolism
Taurine and hypotaurine metabolism	2	L-Glutamate; Taurine	Amino acid metabolism
Glyoxylate and dicarboxylate metabolism	3	DL-Serine; L-Glutamate; L-Glutamine	Carbohydrate metabolism
Sphingolipid metabolism	2	DL-Serine; Sphingosine	Lipid metabolism
Ferroptosis	2	Glutathione disulfide; L-Glutamate	Cell growth and death
Sulfur metabolism	2	DL-Serine; Taurine	Energy metabolism
FoxO signaling pathway	1	L-Glutamate	Signal transduction

Table S4. The identified metabolic pathways that are significantly changed between hypochlorite and control.

Pathway names	Hits	Metabolites	Category
ABC transporters	4	DL-Serine; L-Glutamate; L-Glutamine; Taurine	Membrane transport
Aminoacyl-tRNA biosynthesis	3	DL-Serine; L-Glutamate; L-Glutamine; L-Asparagine	Translation
Biosynthesis of amino acids	5	DL-Serine; L-Glutamate; L-Glutamine; L-Asparagine; L-Citrulline	Global and overview maps
Alanine, aspartate and glutamate metabolism	4	L-Glutamate; L-Glutamine; D-Aspartic acid; L-Asparagine;	Amino acid metabolism
Arginine biosynthesis	3	L-Glutamate; L-Glutamine; L-Citrulline	Amino acid metabolism
Glutathione metabolism	3	Glutathione disulfide; L-Glutamate; L-Pyroglutamic acid	Amino acid metabolism
D-Glutamine and D-glutamate metabolism	2	L-Glutamate; L-Glutamine	Amino acid metabolism
Nitrogen metabolism	2	L-Glutamate; L-Glutamine	Energy metabolism
Taurine and hypotaurine metabolism	2	L-Glutamate; Taurine	Amino acid metabolism
Glyoxylate and dicarboxylate metabolism	3	DL-Serine; L-Glutamate; L-Glutamine	Carbohydrate metabolism
Sphingolipid metabolism	2	DL-Serine; Sphingosine	Lipid metabolism
Ferroptosis	2	Glutathione disulfide; L-Glutamate	Cell growth and death
Sulfur metabolism	2	DL-Serine; Taurine	Energy metabolism
FoxO signaling pathway	1	L-Glutamate	Signal transduction

Table S5. The identified metabolic pathways that are significantly changed between the mixture exposure of CuSNPs and hypochlorite and CuSNPs.

Pathway names	Hits	Metabolites	Category
Arginine biosynthesis	3	Argininosuccinic acid; L-Citrulline; L-Glutamate	Amino acid metabolism
Pyruvate metabolism	3	DL-lactate; DL-lactate; Pyruvaldehyde	Carbohydrate metabolism
Glutathione metabolism	3	Glutathione disulfide; L-Glutamate; L-Pyroglutamic acid	Amino acid metabolism
Gap junction	2	Dopamine; L-Glutamate	Cellular community - eukaryotes
Neuroactive ligand-receptor interaction	3	Dopamine; L-Glutamate; Taurine	Signaling molecules and interaction
Biosynthesis of amino acids	4	Argininosuccinic acid; L-Citrulline; L-Glutamate; L-Histidine	Global and overview maps
ABC transporters	5	Choline; L-Glutamate; L-Histidine; Taurine; Glycerol 3-phosphate	Membrane transport
Taurine and hypotaurine metabolism	2	L-Glutamate; Taurine	Amino acid metabolism
Alanine, aspartate and glutamate metabolism	2	Argininosuccinic acid; L-Glutamate	Amino acid metabolism
Ferroptosis	2	Glutathione disulfide; L-Glutamate	Cell growth and death
beta-Alanine metabolism	2	L-Histidine; Pantothenate	Amino acid metabolism
Histidine metabolism	2	L-Glutamate; L-Histidine	Amino acid metabolism
Propanoate metabolism	2	DL-lactate; Pyruvaldehyde	Carbohydrate metabolism
FoxO signaling pathway	1	L-Glutamate	Signal transduction
Aminoacyl-tRNA biosynthesis	2	L-Glutamate; L-Histidine	Translation
Glycerophospholipid metabolism	3	Choline; Glycerol 3-phosphate; Glycerophosphocholine	Lipid metabolism

Table S6. The identified metabolic pathways that are significantly changed between the mixture exposure of CuSNPs and hypochlorite and hypochlorite.

Pathway names	Hits	Metabolites	Category
ABC transporters	6	Choline; D-Maltose; D-Xylose; Glycerol 3-phosphate; L-Phenylalanine; Taurine	Membrane transport
Glycerophospholipid metabolism	4	Choline; Glycerol 3-phosphate; Glycerophosphocholine; sn-Glycerol 3-phosphoethanolamine	Lipid metabolism
Neuroactive ligand-receptor interaction	3	4-Aminobutyric acid; Taurine; Tyramine	Signaling molecules and interaction
Ether lipid metabolism	2	Glycerophosphocholine; sn-Glycerol 3-phosphoethanolamine	Lipid metabolism
Arginine and proline metabolism	3	4-Aminobutyric acid; Creatine; D-Proline	Amino acid metabolism
Amino sugar and nucleotide sugar metabolism	3	D-Xylose; D-Mannose 1-phosphate; UDP-N-acetylglucosamine	Carbohydrate metabolism